

Technical University of Denmark



Lithium intercalation into layered LiMnO₂

Vitins, G.; West, Keld

Published in:
Electrochemical Society. Journal

Link to article, DOI:
[10.1149/1.1837869](https://doi.org/10.1149/1.1837869)

Publication date:
1997

Document Version
Publisher's PDF, also known as Version of record

[Link back to DTU Orbit](#)

Citation (APA):
Vitins, G., & West, K. (1997). Lithium intercalation into layered LiMnO₂. *Electrochemical Society. Journal*, 144(8), 2587-2592. DOI: 10.1149/1.1837869

DTU Library

Technical Information Center of Denmark

General rights

Copyright and moral rights for the publications made accessible in the public portal are retained by the authors and/or other copyright owners and it is a condition of accessing publications that users recognise and abide by the legal requirements associated with these rights.

- Users may download and print one copy of any publication from the public portal for the purpose of private study or research.
- You may not further distribute the material or use it for any profit-making activity or commercial gain
- You may freely distribute the URL identifying the publication in the public portal

If you believe that this document breaches copyright please contact us providing details, and we will remove access to the work immediately and investigate your claim.

Lithium Intercalation into Layered LiMnO_2

G. Vitins^a and K. West

Department of Chemistry, Technical University of Denmark, DK-2800 Lyngby, Denmark

ABSTRACT

Recently Armstrong and Bruce¹ reported a layered modification of lithium manganese oxide, LiMnO_2 , isostructural with LiCoO_2 . LiMnO_2 obtained by ion exchange from $\alpha\text{-NaMnO}_2$ synthesized in air is characterized by x-ray diffraction and by electrochemical insertion and extraction of lithium in a series of voltage ranges between 1.5 and 4.5 V relative to a lithium electrode. During cycling, voltage plateaus at 3.0 and 4.0 V vs. Li develop, indicating that the material is converted from its original layered structure to a spinel structure. This finding is confirmed by x-ray diffraction. Contrary to expectations based on thermodynamics, insertion of larger amounts of lithium leads to a more complete conversion. We suggest that a relatively high mobility of manganese leaves Li and Mn randomly distributed in the close-packed oxygen lattice after a deep discharge. This isotropic Mn distribution can relatively easily relax to the Mn distribution characteristic of spinels whereas the anisotropic distribution characteristic of layered structures is not reformed when excess lithium is extracted.

Introduction

With the introduction of the lithium-ion battery concept, the "voltage" (potential relative to a lithium electrode) of electrode materials has become an important design parameter. A high voltage of the positive electrode, preferably above 4 V vs. Li, is required in order to minimize the loss in energy density introduced by the nonzero voltage of the coke or graphite used as negative electrode. High voltages can be found in two groups of intercalation materials: in layered lithium transition metal dioxides (e.g., LiCoO_2 and LiNiO_2) and in lithium transition metal spinels, especially LiMn_2O_4 . These materials have "unusually" high voltages, i.e., voltages that are considerably higher than known from materials with similar compositions, but different structures. The high voltage of the layered oxides stems from a destabilization of the host structure caused by lithium extraction. This can be illustrated by the fact that lithium extraction from the ideally layered LiCoO_2 occurs at a considerably higher voltage compared to lithium extraction from disordered LiCoO_2 ,² where interlayer transition metal ions reduce the electrostatic repulsion between negatively charged oxide layers. This destabilization eventually leads to irreversible structural breakdown if a critical limit of lithium extraction is exceeded. The high voltage of lithium extraction from the manganese spinel can be ascribed to the oxygen coordination of lithium in this structure. The tight tetrahedral coordination offered by the spinel structure defines a particularly stable environment for lithium ions, resulting in higher potentials during lithium insertion or extraction than in materials with octahedral coordination. The tetrahedral sites in most other close-packed structures used as intercalation hosts share faces with octahedral sites occupied by transition metal ions. These sites are energetically disfavored for electrostatic reasons. The current efforts in the investigations on new electrode materials with high energy density are focused on alternative materials with similar or better performance compared to LiCoO_2 ,³ LiNiO_2 ,⁴ or $\text{Li}_{1-x}\text{Mn}_{2-x}\text{O}_4$.⁵⁻⁷ A point of special concern is to find materials with an initial lithium capacity larger than the, at best, 160 mAh/g offered by these materials. Cost and environmental issues are also of concern, making manganese-based materials much more attractive than e.g., cobalt oxides. Orthorhombic LiMnO_2 is such a material; it exists both in a low-temperature modification with an initial charge capacity close to 230 mAh/g,⁸⁻¹⁰ and in a high-temperature modification with an initial charge capacity of 150 mAh/g.^{11,12} Upon cycling, these materials transform into spinel-like materials,^{9,10,12,13} but they do not exhibit the good cycling performance that can be achieved with optimized lithium manganese spinels.

Recently a new layered LiMnO_2 compound analogous to LiCoO_2 was reported by Armstrong and Bruce.¹ This mate-

rial is not thermodynamically stable, but could be obtained by an ion-exchange reaction where $\alpha\text{-NaMnO}_2$ was refluxed with LiCl or LiBr in *n*-hexanol for 6 to 8 h at 150°C. A previous attempt to perform similar ion-exchange reactions was not successful¹⁴: refluxing with LiCl in methanol for 32 h gave an incomplete ion exchange, whereas the reaction in molten LiI at about 450°C resulted in complete exchange of Na with Li, but the product did not retain the layered structure of the starting material. The product phase was identified as isotopic with the lithium insertion product of the spinel LiMn_2O_4 . This insertion product, $\text{Li}_2\text{Mn}_2\text{O}_4$ has a spinel-related ordered rock salt structure.¹⁵⁻¹⁷

The structure of layered LiMnO_2 was established by neutron powder diffraction to be monoclinic with space group C2/m and unit cell dimensions: $a = 5.4387(7)$, $b = 2.80857(4)$, $c = 5.3878(6)$ Å, $\beta = 116.006(3)^\circ$.¹ Lithium ions are located in octahedral sites between MnO_6 -octahedron sheets. The oxygen packing is not regular due to a Jahn-Teller distortion.

In this paper we examine the electrochemical properties of the layered lithium manganese oxide. By analysis of the differential capacities obtained during galvanostatic cycling of Li/LiMnO₂ cells we show that this material is unstable towards lithium extraction/insertion and transforms into a spinel-related modification just like the orthorhombic material does on cycling.²⁶ We also discuss aspects of the synthesis of the layered lithium manganese oxide.

Experimental

Synthesis of the metastable layered lithium manganese dioxide is performed in two steps: synthesis of $\alpha\text{-NaMnO}_2$ and exchange of sodium ions with lithium ions under soft chemistry conditions. At each step in the synthesis, the phase contents of the samples were analyzed by x-ray powder diffraction carried out on a Phillips automated powder diffractometer, PW1710, using Cu K α radiation and W as an internal standard.

Synthesis of $\alpha\text{-NaMnO}_2$.— $\alpha\text{-NaMnO}_2$ was synthesized from Na_2CO_3 and MnCO_3 heated to 700 to 710°C under flowing nitrogen for 18 h with an intermediate grinding.^{13,14} As $\alpha\text{-NaMnO}_2$ has been reported to be stable in oxygen above 650°C,¹⁸ a simpler synthetic route was tried. A batch of the same starting materials was heated twice to 725°C in air for 24 h and then quenched to room temperature. Between these two firings the product was finely ground in a mortar.

Ion exchange.—The ion exchange was performed by heating $\alpha\text{-NaMnO}_2$ in a solution of lithium bromide in *n*-hexanol (4 M) to 145 to 154°C for 8 h or 24 h. After this period, the slurry was filtered, and the precipitate washed with *n*-hexanol and methanol. The total amount of LiBr corresponds to a five to tenfold excess of the amount required for full exchange of Na with Li. LiBr was found

^a Permanent address: Institute of Solid State Physics, University of Latvia, LV-1063 Riga, Latvia.

to be well suited for this purpose, as it is highly soluble in *n*-hexanol whereas the NaBr formed in the reaction is only poorly soluble but dissolves easily in methanol.

Electrochemical testing.—For galvanostatic cycling, electrodes were made as composite films containing 60% by weight lithium manganese oxide, 10% carbon (Ketjen EC Black), and 30% polyethylene oxide (PEO, $M_w \approx 4 \times 10^6$) used as an ionically conducting binder. The electrode films were solvent cast onto aluminum foil and punched into circular disks (1 cm diam each containing 1 to 2 mg active material). The exact amount of manganese oxide was determined by chemical analysis after cycling. To eliminate traces of water, the electrode disks were dried in vacuum at 100 to 120°C for 20 h prior to use.

The electrodes were cycled in spring-loaded test cells with metallic lithium as the negative electrode and an electrolyte consisting of LiPF_6 (1 M) dissolved in a 1:1 mixture of ethylene carbonate and diethyl carbonate. Porous polypropylene sheets (Celgard 2400) were used as separators.

As in our previous work, we used galvanostatic discharge and charge to fixed voltage limits followed by a period of potentiostatic charging at the upper voltage in order to bring the electrode to a reproducible state before each discharge. The differential capacity (dx/dE) is calculated numerically from the voltage/time relationship and the amount of oxide in the electrode. Currents in the range 10 to 25 μA , corresponding to discharge times larger than 10 h/ x , were chosen in order to minimize concentration polarization effects. At lower currents, a systematic imbalance between the capacities during charge and discharge due to parasitic reactions with electrolyte impurities became noticeable. The results obtained with the layered lithium manganese oxide are compared with results obtained under identical conditions with a well-characterized lithium manganese spinel, LiMn_2O_4 obtained from Sedema, Tertre, Belgium.

Results and Discussion

Synthesis of $\alpha\text{-NaMnO}_2$.—X-ray diffraction of the yellowish brown powders resulting from either synthetic route to $\alpha\text{-NaMnO}_2$ confirmed the presence of the correct monoclinic phase. The powder synthesized under nitrogen showed additional diffraction lines (relative intensity less than 5%) from the orthorhombic NaMnO_2 β -phase. The lattice constants of the two powders are compared with literature data in Table I.

It is seen that there is a tendency for an increased unit cell volume for samples obtained in nitrogen atmosphere, consistent with a reduction of the average oxidation state of manganese slightly below the ideal value of 3.0. The lattice constants of the sample prepared in air are closer to the single-crystal data¹⁹ obtained on a sample prepared in a closed system. The differences are small, however. Literature data^{12,15,19} suggest that the oxidation state of Mn in this phase can vary only in a narrow interval: 2.95 to 3.08.

Upon exposure to humid air, the color of the powders changes from yellowish brown to dark brown. It seems that $\alpha\text{-NaMnO}_2$ initially reacts with moisture to form a sodium-deficient product with an intense diffraction line at $d = 5.57 \text{ \AA}$ corresponding to x-ray diffraction (XRD) data for $\alpha\text{-Na}_{0.70}\text{MnO}_{2+y}$.²⁰ After a longer exposure to humid air, $\alpha\text{-NaMnO}_2$ is converted to a black powder having an ill-

defined diffraction pattern that could not be indexed to the parent phase.

Synthesis of LiMnO_2 .—Chemical analysis of the brown powder obtained after the ion-exchange reaction on either of the two $\alpha\text{-NaMnO}_2$ preparations showed that the lithium exchange was nearly complete, with a $[\text{Na}]/[\text{Li}]$ ratio of 7%. X-ray diffraction confirmed that the product had the layered lithium manganese oxide structure. The few diffraction lines that did not belong to this material were of a relative intensity less than 5%. Particularly at low angles there was an unidentified line ($d = 6.66 \text{ \AA}$) that was also observed in a previous investigation.²¹ The unit cell parameters of the product ($a = 5.431(6) \text{ \AA}$, $b = 2.809(2) \text{ \AA}$, $c = 5.390 \text{ \AA}$, and $\beta = 115.95(7)^\circ$)^b as determined from least squares refinement were consistent with the values given in the literature.^{1,21}

Electrochemical cycling.—Cycling of the layered LiMnO_2 in the potential range between 3.0 and 4.5 V vs. Li is shown in Fig. 1. In the first charge, lithium is extracted over a plateau at 4.1 V vs. Li to $x = 0.3$, where x is the composition parameter in Li_xMnO_2 . Some cells show an even larger capacity in the first charge, but as this capacity is not correlated to the capacity in subsequent cycles, we believe that this additional capacity is due to electrolyte decomposition on an incompletely passivated electrode. During subsequent cycling, the capacity is considerably smaller than in the first charge, and fades relatively quickly upon repeated cycling. This is similar to the cycling performance given by Armstrong and Bruce.¹ The major part of the capacity is found in a quasi plateau centered around 4 V as is seen from the differential capacity curves for cycles 2 and 3 in Fig. 1. Even at the relatively low rate used here for cycling, the hysteresis between the discharge voltage and the charge voltage is much larger (0.3 to 0.4 V) than expected for a typical intercalation reaction where lithium ions are inserted into or removed from galleries occupied only by mobile guest ions.

Attempting to increase the capacity, the lower limiting voltage was extended to 2.0 V vs. Li. Results of cycling in the voltage range between 2.0 and 4.5 V are shown on Fig. 2. In this particular cell it is clear that a large part of the capacity during the first charge is due to electrolyte decomposition as the capacity exceeds the amount of lithium initially present in the oxide. Furthermore, the voltage shows a local minimum characteristic of an autocatalytic process. This phenomenon is absent from the voltage curves obtained during cycling of other manganese oxides under identical conditions, and we suppose it to originate from an instability of the electrolyte at high voltage catalyzed by the surface of manganese oxide particles, which remain active during the conformation change. A similar effect is known to occur during a phase change of MoS_2 induced by lithium insertion.²² In most cases the plateau associated with electrolyte decomposition is only seen in the first charge, but in a few instances it may be present in the second charge as well, see Fig. 2. When cycled in this range two plateaus on the voltage curve or two sets of peaks in differential capacity are seen, one centered around 4.0 V and one around 3.0 V. The capacity retention on cycling is better and the voltage hysteresis less than in cells

^b Determined on the product of ion exchange of the α -exchange of the $\alpha\text{-NaMnO}_2$ sample made in air.

Table I. Lattice parameters of $\alpha\text{-NaMnO}_2$.

	Fuchs <i>et al.</i> ¹⁴ Synthesis in nitrogen	Jansen <i>et al.</i> ¹⁹ Single crystal, synthesis in a closed system	This work Synthesis in nitrogen	This work Synthesis in air
<i>a</i>	5.678(5) \AA	5.662 \AA	5.672(1) \AA	5.663(1) \AA
<i>b</i>	2.853(3) \AA	2.860 \AA	2.8607(4) \AA	2.8597(4) \AA
<i>c</i>	5.811(5) \AA	5.799 \AA	5.804(1) \AA	5.804(1) \AA
β	113.2(1) ^o	113.10 ^o	113.14(2) ^o	113.13(2) ^o
<i>V</i>	86.67 \AA^3	86.38 \AA^3	86.60 \AA^3	86.43 \AA^3

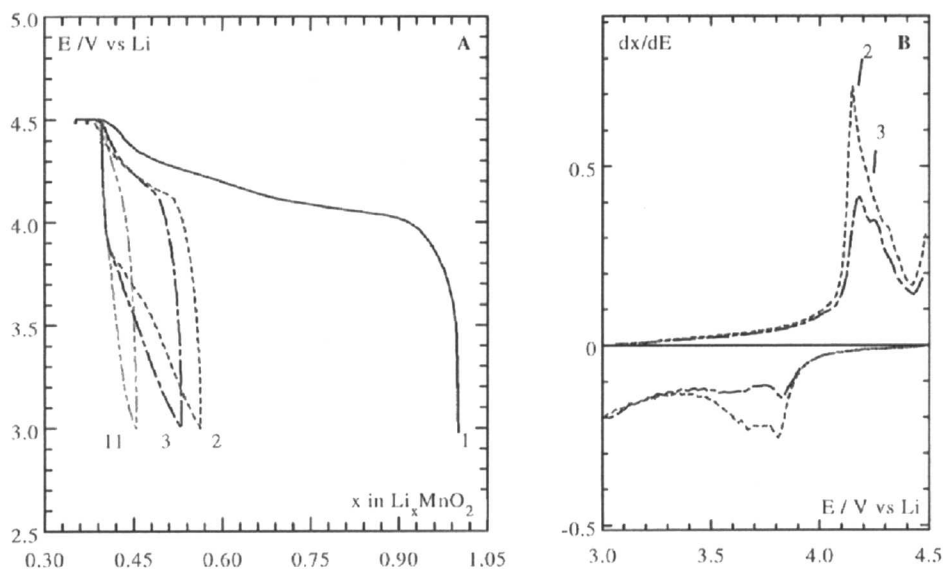


Fig. 1. (A) Potential (E) vs. composition (x), and (B) differential capacity (dx/dE) vs. potential for lithium extraction and re-insertion in Li_xMnO_2 . Data or different cycles are shown as indicated on the graph. Discharge/charge current $13 \mu\text{A}/\text{cm}^2$, corresponding to a discharge time of $24 \text{ h}/x$.

discharged only to 3.0 V. The reversible capacity, however, still only involves half the amount of lithium originally present in the structure.

After termination of the cycling experiments, electrodes were examined by x-ray diffraction. Diffraction patterns of electrodes cycled in the intervals 3.0 to 4.5 V, and 2.4 to 4.0 V are compared with patterns of the pristine layered lithium manganese oxide and a lithium manganese oxide spinel in Fig. 3. The polypropylene separator used as carrier for the cycled electrode material gives rise to additional lines at low angles (marked with P on the figure). It is seen that the cycled electrodes show the weak, broad diffraction peaks characteristic of poorly crystalline materials, and that the peaks change position and resemble the spinel pattern more than the pattern characteristic of the original layered oxide. This does not necessarily imply that the structure changes to a spinel structure, because a fortuitous incidence makes it impossible by diffraction methods to distinguish between a slightly distorted layered LiMnO_2 structure (the "cubic layered structure") and a lithiated spinel $\text{Li}_2\text{Mn}_2\text{O}_4$.²³ However, the presence of peaks at both 4.0 V vs. Li and at 3.0 V vs. Li in the capacity curve of the cycled material show that two essentially

different types of lithium sites are present. This is not expected for a layer structure, but is characteristic of a spinel having two sets of sites available for lithium insertion, both octahedral sites and a set of tetrahedral sites not sharing faces with occupied octahedra. For comparison, voltage and capacity curves obtained from cycling of a lithium manganese oxide spinel (from Sedema) in the voltage range (1.0 to 4.5 V vs. Li) are shown in Fig. 4. Basically the spinel has capacity in plateaus at 3 and 4 V vs. Li with the 4 V plateau showing a characteristic splitting. Cycling in this extended range leads to characteristic changes in the voltage profile of this otherwise very stable electrode material.

In order to avoid the ambiguities introduced by the irreversible electrolyte reaction in the first charge, a series of experiments was conducted with the charging voltage limited to 4.0 V vs. Li. Fig. 5 shows results from such an experiment. On the initial charge, an equivalent of 0.3 Li per Mn could be extracted. In the subsequent cycles between 2.9 and 4.0 V vs. Li only a fraction of this capacity could be cycled and the amount decreased further upon cycling. After ten of these cycles the lower voltage limit was decreased to 2.5 V vs. Li, resulting in a gradual

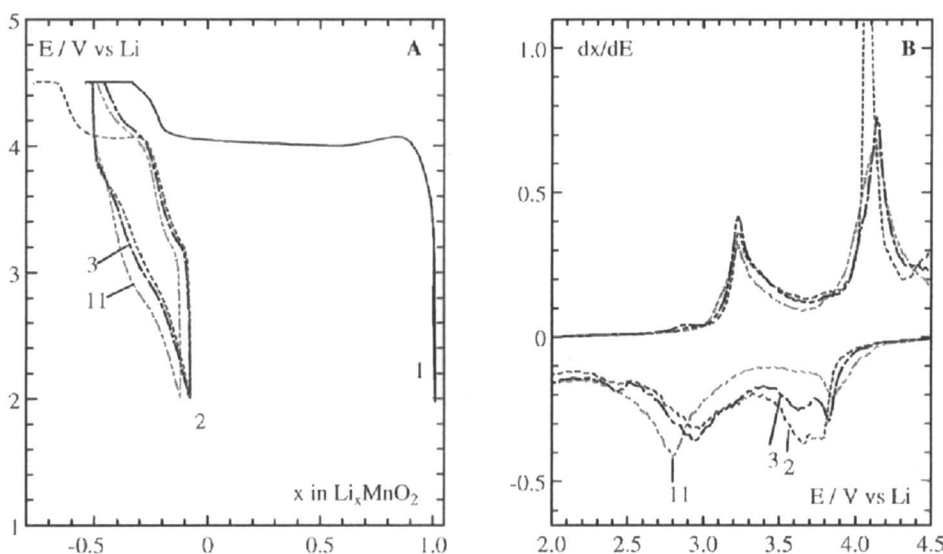
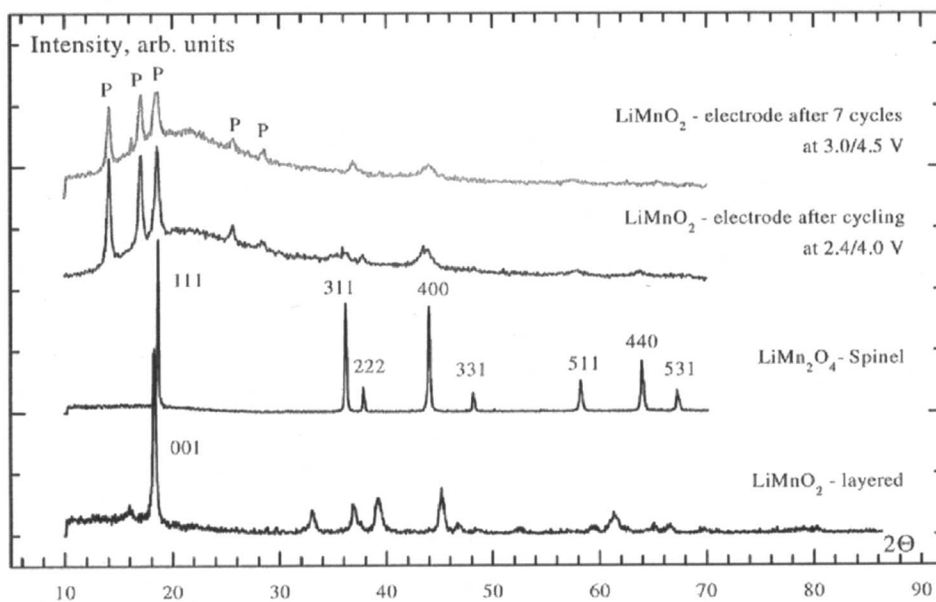


Fig. 2. (A) Potential (E) vs. composition (x), and (B) differential capacity (dx/dE) vs. potential for cycling of Li_xMnO_2 . Discharge/charge current $13 \mu\text{A}/\text{cm}^2$, corresponding to a discharge time of $15 \text{ h}/x$.

Fig. 3. X-ray diffractograms of electrodes cycled in different potential intervals compared with diffractograms of the pristine layered LiMnO_2 and the spinel LiMn_2O_4 . Diffraction line marked with P originates from the polypropylene separator.

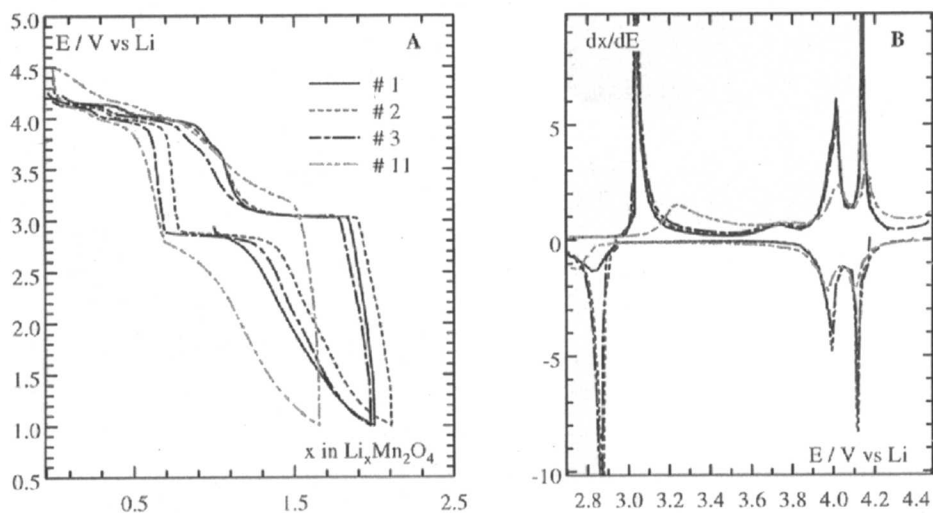


increase in the cycling capacity. The major part of this new capacity is found in a voltage plateau centered around 3.0 V, but as the capacity in this region increases, a new set of capacity peaks emerges just below 4 V *vs.* Li. This behavior is similar to the behavior shown by the spinel LiMn_2O_4 when cycled in the same voltage range, a similarity that is further enhanced as the minimum voltage is decreased further. Fig. 6 shows the 61st cycle of a LiMnO_2 electrode which up to cycle 60 was cycled between 4.0 V and a minimum voltage gradually decreased to 1.5 V. During this treatment the capacity increased to an equivalent of 0.4 Li per Mn. Increasing the upper voltage to 4.5 V further increased the cycling capacity to more than one Li per Mn, and the differential capacity curve now shows the split set of peaks at 4 V characteristic of the spinel. The peak at 3.74 V on charge was also observed in spinels cycled in a wide voltage range (see Fig. 4 and Ref. 7) but is more pronounced in this preparation. Presently we have no explanation for this peak, but know that it is correlated to the appearance of additional capacity below 3 V. The XRD on this electrode after completion of the cycling experiment showed no diffraction lines; the product was amorphous to x-rays.

Conclusions

Lithium extraction from and reinsertion into the layered lithium manganese oxide is not a reversible intercalation reaction. Unlike the isostructural nickel and cobalt oxides, LiNiO_2 and LiCoO_2 , the manganese oxide undergoes a structural breakdown after a small amount of lithium is extracted. Cycling of this material in the voltage range where the initial lithium extraction takes place only involves a very small capacity, whereas cycling to low voltages promotes a structural rearrangement to a spinel-related modification that cycles much better than the pristine material, although it never reaches the capacity of the pure spinel material. The conversion to a spinel-like material is apparently paradoxical, as the spinel phase is thermodynamically stable only at compositions near $\text{Li}/\text{Mn} \approx 0.5$ whereas it is orthorhombic LiMnO_2 , having a layer structure with a double stack of edge-sharing MnO_6 octahedra, that is stable at a higher lithium content. A key to the understanding of this paradox is that a random distribution of lithium and manganese in a cubic close-packed array of oxygen ions is much closer to the spinel structure than to a layered structure. The stresses induced

Fig. 4. (A) Potential (E) vs. composition (x), and (B) differential capacity (dx/dE) vs. potential for cycling of $\text{Li}_x\text{Mn}_2\text{O}_4$ (Sedema). Discharge/charge current $13 \mu\text{A}/\text{cm}^2$, corresponding to a discharge time of 3.3 h/ x .



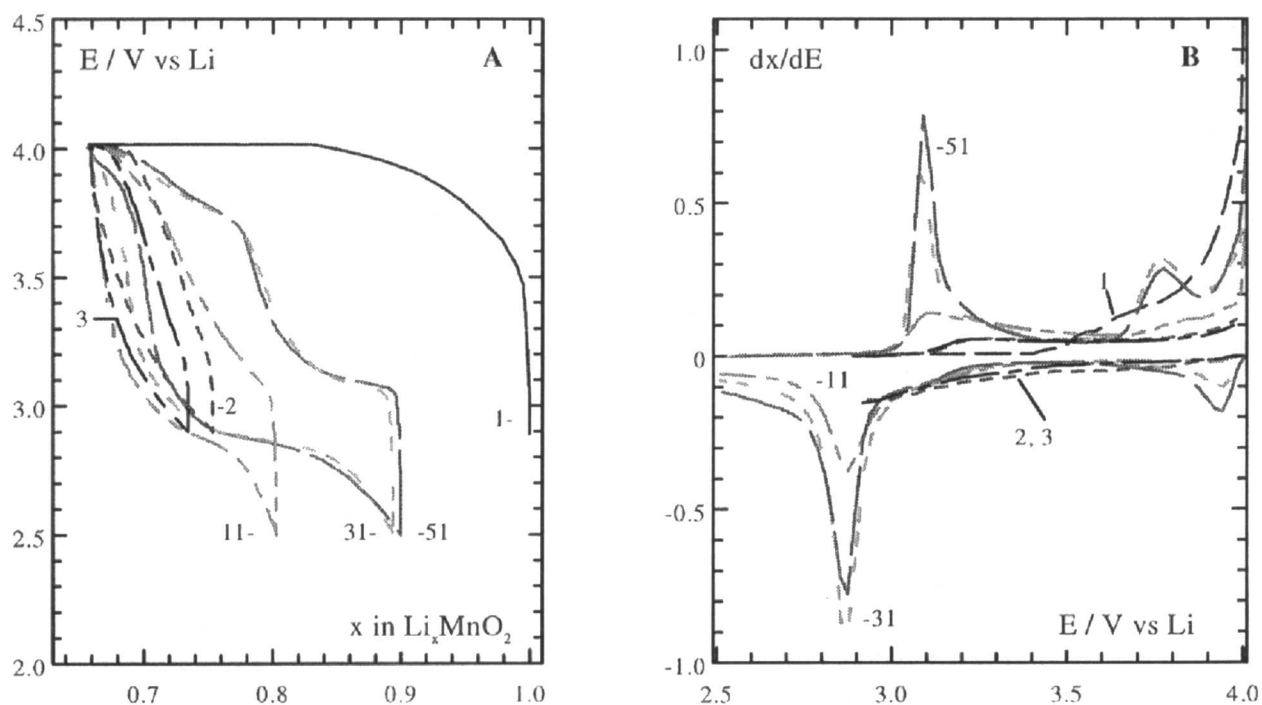


Fig. 5. (A) Potential (E) vs. composition (x), and (B) differential capacity (dx/dE) vs. potential for cycling of Li_xMnO_2 . Discharge/charge current $25 \mu\text{A}/\text{cm}^2$, corresponding to a discharge time of 14 h/x.

by a high degree of lithium insertion combined with a relatively high mobility of manganese ions in an oxide lattice²⁴ frustrates the structure and causes a displacement of manganese ions from their original positions. After a number of cycles, a certain degree of randomness in distribution of manganese ions is the result. The spinel structure representing a uniform, isotropic distribution of manganese ions in a close-packed oxygen lattice thus repre-

sents a local energy minimum that is more easily attained under dynamic conditions than, *e.g.*, the orthorhombic structure.

The mechanism suggested above also explains why cycling of the orthorhombic layered LiMnO_2 leads to transformation of the oxide to a spinel-like material.^{9,10,12,13} The implied high mobility of manganese in an oxide framework makes it unlikely that a lithium manganese

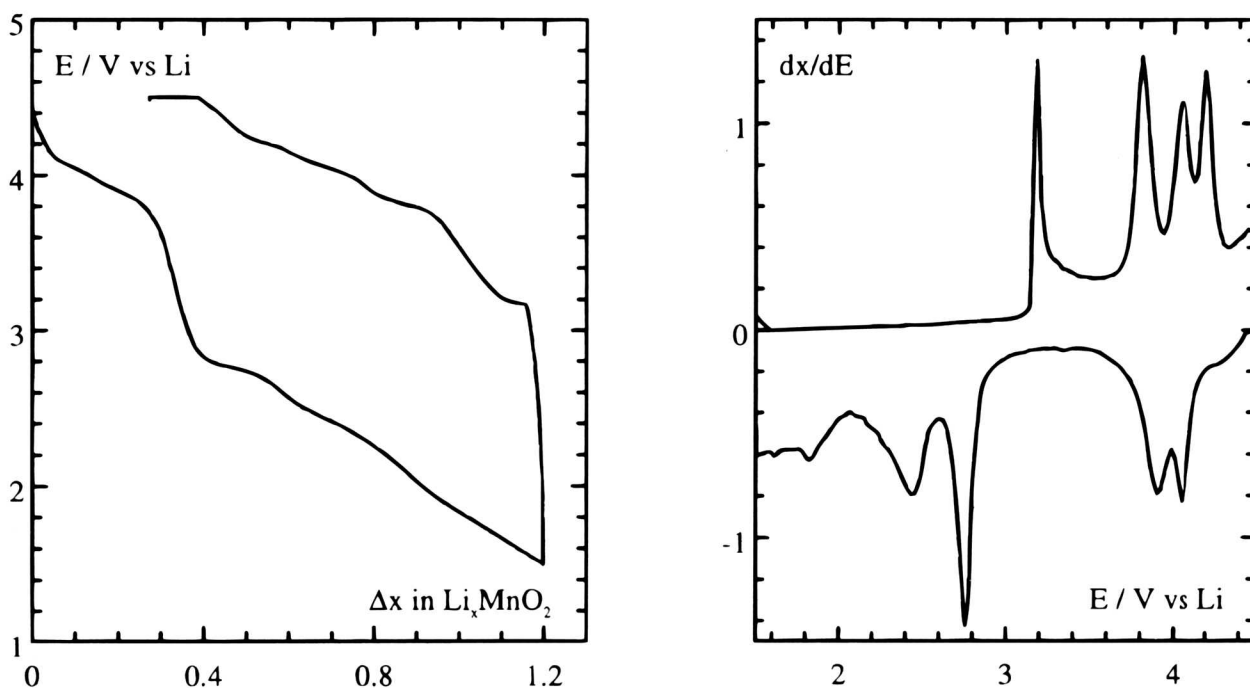


Fig. 6. (A) Potential (E) vs. composition (x), and (B) differential capacity (dx/dE) vs. potential for cycling of Li_xMnO_2 . Discharge/charge current $13 \mu\text{A}/\text{cm}^2$, corresponding to a discharge time of 10.5 h/x.

oxide with a reversible high-voltage capacity much larger than that of LiMn_2O_4 will be found. In most lithium manganese oxides, lithium insertion into octahedral sites with simultaneous reduction of Mn(IV) to Mn(III) occurs at a voltage just above 3.0 V vs. Li.²⁵ A higher voltage can be obtained if lithium is accommodated on tetrahedral sites, but in hexagonal close-packed structures the amount of tetrahedral sites not sharing faces with occupied octahedra is limited to the AB_2O_4 composition. Alternatively, a higher voltage could be obtained if lithium extraction results in a large change in the stability of the MnO framework, as in layered oxides. But due to the high mobility of Mn, such changes in stability will induce Mn motion and cause a breakdown of the host structure.

Acknowledgments

A scholarship from The Danish Rectors Conference to G.V. is gratefully acknowledged. Sedema is thanked for their kind supply of lithium manganese spinel.

Manuscript submitted Jan. 31, 1997; revised manuscript received April 15, 1997.

Technical University of Denmark assisted in meeting the publication costs of this article.

REFERENCES

1. A. R. Armstrong and P. G. Bruce, *Nature*, **381**, 499 (1996).
2. R. J. Gummow and M. M. Thackeray, *Solid State Ionics*, **53-56**, 681 (1992).
3. J. N. Reimers and J. R. Dahn, *This Journal*, **139**, 2091 (1992).
4. J. R. Dahn, U. von Sacken, M. W. Juzkow, and H. Al-Janaby, *ibid.*, **138**, 2207 (1991).
5. R. J. Gummow and A. K. Thackeray, *Solid State Ionics*, **69**, 59 (1994).
6. J. M. Tarascon and D. Guyomard, *Electrochim. Acta*, **38**, 1221 (1993).
7. J. Barker, K. West, Y. Saidi, R. Punenborg, B. Zachau-Christiansen, and R. Koksang, *J. Power Sources*, **54**, 475 (1995).
8. T. Ohzuku, A. Ueda, and T. Hirai, *Chem. Express*, **7**, 193 (1992).
9. J. N. Reimers, E. W. Fuller, E. Rossen, and J. R. Dahn, *This Journal*, **140**, 3396 (1993).
10. I. Koetschau, M. N. Richard, J. R. Dahn, J. B. Soupart, and J. C. Rousche, *ibid.*, **142**, 2906 (1995).
11. R. Hoppe, G. Brachtel, and M. Jansen, *Z. Anorg. Allg. Chemie*, **417**, 1 (1975).
12. I. J. Davidson, R. S. McMillian, J. J. Murray, and J. E. Greedan, *J. Power Sources*, **54**, 232 (1995).
13. R. J. Gummow, D. C. Liles, and M. M. Thackeray, *Mater. Res. Bull.*, **28**, 1249 (1993).
14. B. Fuchs and S. Kemmler-Stack, *Solid State Ionics*, **68**, 279 (1994).
15. M. M. Thackeray, W. I. F. David, P. G. Bruce, and J. B. Goodenough, *Mater. Res. Bull.*, **18**, 416 (1983).
16. A. Mosbah, A. Verbaere, and M. Tornoux, *ibid.*, **18**, 1375 (1983).
17. J. M. Tarascon and D. Guyomard, *This Journal*, **138**, 2864 (1991).
18. R. Scholder and U. Protzer, *Z. Anorg. Allg. Chemie*, **369**, 313 (1969).
19. M. Jansen and R. Hoppe, *ibid.*, **399**, 163 (1973).
20. J.-P. Parant, R. Olazcuaga, M. Devalette, C. Fouassier, and P. Hagenmuller, *J. Solid State Chem.*, **3**, 1 (1971).
21. F. Capitaine, P. Gravereau, and C. Delmas, *Solid State Ionics*, **89**, 197 (1996).
22. J. A. R. Stiles and D. T. Fouchard, in *Primary and Secondary Ambient Temperature Lithium Batteries*, J. P. Gabano, Z. Takahara, and P. Bro, Editors, PV 88-6, p. 422, The Electrochemical Society Proceedings Series, Pennington, NJ (1988).
23. J. N. Reimers, W. Li, E. Rossen, and J. R. Dahn, *Mater. Res. Soc. Symp. Proc.*, **293**, 3 (1993).
24. W. I. F. David, M. M. Thackeray, P. G. Bruce, and J. B. Goodenough, *Mater. Res. Bull.*, **19**, 99 (1984).
25. B. Zachau-Christiansen, K. West, T. Jacobsen, S. Skaarup, *Solid State Ionics*, **70/71**, 401 (1994).
26. Similar results have recently been reported by C. Delmas and F. Capitaine, in Extended Abstracts No. II-B-33, p. 470 of the 8th International Meeting on Lithium Batteries, Nagoya, The Electrochemical Society of Japan (1996).